This is the peer reviewed version of the following article: Vratarić M, Šenk V, Bursać B, Gligorovska L, Ignjatović D, Kovačević S, Veličković N, Djordjevic A. Fructose diet ameliorates effects of macrophage migration inhibitory factor deficiency on prefrontal cortex inflammation, neural plasticity, and behavior in male mice. Biofactors. 2021, which has been published in final form at http://dx.doi.org/10.1002/biof.1802.

Fructose diet ameliorates effects of macrophage migration inhibitory factor deficiency on prefrontal cortex inflammation, neural plasticity and behavior in male mice

Miloš Vratarić[1], Vladimir Šenk[1], Biljana Bursać[1], Ljupka Gligorovska[1], Djurdjica Ignjatović[1], Sanja Kovačević[1], Nataša Veličković[1], Ana Djordjevic[1]*

[1]Institute for Biological Research "Siniša Stanković"- National Institute of Republic of Serbia, Department of Biochemistry, University of Belgrade, Belgrade, Serbia

Running title: Fructose and inflammation in MIF-KO mice prefrontal cortex

*Corresponding author: Ana Djordjevic, PhD

Abbreviations: macrophage migration inhibitory factor (MIF); interleukin-1β (IL-1β); tumor necrosis factor-α (TNF-α); toll-like receptor 4 (TLR-4); arginase 1 (Arg-1); mannose receptor (MRC-1); leukemia inhibitory factor (LIF); glycogen synthase kinase-3 (GSK-3); protein kinase C (PKC); phosphorylated insulin receptor substrate 1 (pIRS-1); AMP-activated protein kinase α (AMPKα); brain derived neurotrophic factor (BDNF); insulin-like growth factor 1 (IGF-1); calcium calmodulin dependent kinase 2 alpha (CaMKIIα); glucocorticoid receptor (GR); 11β-hydroxysteroid dehydrogenase type 1 (11β-HSD1); nuclear factor κB (NF-κB); activator protein 1 (AP1); prefrontal cortex (PFC); homeostatic model assessment of insulin resistance (HOMA-IR); quantitative insulin sensitivity check index (QUICKI); fructose 1,6-bisphosphate (FBP).

Department of Biochemistry, Institute for Biological Research "Siniša Stanković" – National Institute of Republic of Serbia, 142 Despot Stefan Blvd., 11000 Belgrade, Serbia

Phone: +381 11 207 83 03; Fax: +381 11 276 14 33; E-mail: djordjevica@ibiss.bg.ac.rs

Abstract

Macrophage migration inhibitory factor (MIF) is a pro-inflammatory cytokine that represents a link between diet-induced inflammation and insulin resistance. Our aim was to examine whether fructose diet affects inflammation and insulin signaling in the prefrontal cortex (PFC) of *Mif* knockout mice (MIF-KO), and their possible link to neural plasticity and behavior. We analyzed nuclear factor κB (NF-κB) and glucocorticoid signaling, expression of F4/80, IL-1β, TNF-α, TLR-4, MyD88, arginase 1 (*Arg-1*), mannose receptor (*Mrc-1*) and leukemia inhibitory factor (*Lif*) to asses inflammation in the PFC of C57/BL6J and MIF-KO mice consuming 20% fructose solution for 9 weeks. Insulin receptor (IR), IRS-1 serine phosphorylations (307 and 1101) and activity of PKCα, Akt, GSK-3β and AMPKα were used to analyze insulin signaling. Brain derived neurotrophic factor (BDNF) and insulin-like growth factor 1 (IGF-1) mRNA levels, together with synapthophysin and PSD-95 protein level and calcium calmodulin dependent kinase 2 (CaMKII) activity, were used as plasticity markers. Behavior was examined in elevated plus maze, light dark box and novel object recognition test. The results showed concomitant increase of *Tnf-α, Tlr-4, MyD88* and M2 microglia markers (*Arg-1, Mrc-1, Lif*) in the PFC of MIF-KO, paralleled with unchanged glucocorticoid and insulin signaling. Increase of BDNF and IGF-1 was paralleled with increased CaMKII activity, decreased PSD-95 protein level, anxiogenic behavior and impaired memory in MIF-KO mice. Fructose feeding restored these parameters in the PFC

to the control level and mitigated behavioral changes suggesting that ameliorating effects of fructose on neuroinflammation and behavior depend on the presence of MIF.

Keywords: fructose; inflammation; macrophage migration inhibitory factor; prefrontal cortex; neural plasticity; insulin resistance; behavior

1. Introduction

Fructose consumption is an important factor for the development of type 2 diabetes, not only through metabolic disturbances in the liver and adipose tissue, but also through development of insulin resistance in the central nervous system (CNS) (1). It was previously shown that fructose-induced obesity and type 2 diabetes are associated with poorer cognitive performance, cognitive decline and dementia (2, 3), which points the interest to the prefrontal cortex (PFC), a limbic structure involved in higher cognitive functions and anxiety control (4). Several potential mechanisms of cognitive decline in metabolic disturbances have been revealed so far, including hypothalamic and hippocampal inflammation and insulin resistance, while PFC is yet to be investigated (5). In addition, metabolic processing of fructose leads to decreased amount of cellular ATP, sensed by AMP-activated protein kinase (AMPK) (6), which can lead to excessive production of pro-inflammatory cytokines and exacerbation of insulin resistance, also at the level of the CNS (7).

The macrophage migration inhibitory factor (MIF) is a pleiotropic pro-inflammatory cytokine which forms a link between inflammation and insulin resistance (8, 9). Generally, the role of MIF in inflammation is associated with positive regulation of pro-inflammatory cytokines, tumor necrosis factor-α (TNF-α) and interleukin-1β (IL-1β) (10), and with positive regulation of toll-like receptor 4 (TLR-4) (11), which is regulated through activity of proinflammatory kinases such as mitogen-activated protein (MAP) kinase family, as well as the nuclear factor κB (NF-κB) and activator protein 1 (AP1). MIF knockout (MIF-KO) mice generally exert strong anti-inflammatory phenotype, since their activated lymph node cells secrete lower amounts of some pro-inflammatory mediators such as IL-1β, IL-6, IL-23 and

TGF-β, but they, however, secrete higher amounts of TNF-α (12). In addition, in the infarcted myocardium of MIF-KO mice, reduced gene expression of pro-inflammatory cytokines and mediators was observed, whereas anti-inflammatory cytokine IL-10 was up-regulated (13). It has been previously reported that MIF and glucocorticoids can have counter regulating effects on immune cell activation and cytokine production (14) and glucocorticoids are traditionally recognized as suppressors of inflammation (15). Glucocorticoids can be locally produced within the tissues by the enzyme 11β-hydroxysteroid dehydrogenase type 1 (11β-HSD1) (16) and their effects are mediated by the glucocorticoid receptor (GR), a hormone-dependent transcription factor (17). GR transcriptional activity partially depends on post-translational modifications, such as phosphorylation, among which phosphorylation at serine 220 of mouse GR is considered activatory (18). It seems that homeostatic balance between MIF and glucocorticoids is especially important in the brain, determining whether to promote immune responses (in infection) or dampen them (to protect from the harmful effects of inflammation) (19). Still, the exact role of MIF in brain inflammation is largely unclear and although it has a potent pro-inflammatory activity in other organs, it might have quite opposite role in the CNS, as its involvement in detoxification of catecholamine neurotransmitters metabolism has been confirmed (20).

The source of inflammation in the brain can be microglial cells as the resident macrophages of CNS or the macrophages infiltrating from the periphery (21). The general function of adult brain microglia is monitoring of the environment and elicitation of inflammatory response in case of the detection of any danger signal. This leads to M1 activation of microglia and subsequent release of pro-inflammatory cytokines such as TNFα,

IL-6 and IL-1β (22). In the steady state microglia express markers typically present on many other tissue macrophages and/or monocytes, such as F4/80, a glycoprotein found on the surface of macrophages and resting microglia (23). However, microglia also have protective functions when switched to M2 phenotype, as it can release anti-inflammatory cytokines, growth factors (such as insulin-like growth factor 1, IGF-1) and promote trophic support by secretion of neurotrophins like brain derived neurotrophic factor (BDNF) (24). This "alternative" activation microglia is associated with the expression of arginase 1 (Arg-1) and mannose receptor (MRC-1), both of which represent relatively straightforward markers of M2 microglial phenotypes (25, 26). In addition, several authors have reported that certain cytokines, such as leukemia inhibitory factor (LIF), can alter the phenotype of microglia from pro-inflammatory to anti-inflammatory state and even promotes survival of neurons and glia in several animal models (27). The major mediators of inflammation, like IL-1β and TNF-α, are also involved in the development of insulin resistance in the local brain tissues (7) through multiple signaling cascades ending with NF-κB and/or c-Jun N-terminal kinase (JNK) activation (28). At the cellular level, insulin resistance is reflected in the inability to pass the insulin signal through insulin signaling cascade (29). Namely, excessive phosphorylation of serine 307 and 1101 on the insulin receptor substrate 1 (IRS-1) protein reduces its ability to activate downstream PI3 kinase (PI3K) and leads to its accelerated degradation (30). Therefore, the phosphorylation of IRS-1 protein on these serine residues is considered a key marker of cellular insulin resistance (31). Downstream of the PI3K-Akt pathway, insulin signaling also involves glycogen synthase kinase-3 (GSK-3), an enzyme whose activity is down-regulated by serine phosphorylations (32). One of the important players is protein

kinase C (PKC), which may also contribute to insulin resistance by phosphorylating the IRS-1 required for insulin signaling (33). In addition to the IRS proteins, reduced activity of Akt is also associated with the onset of insulin resistance (34, 35). It is interesting that Akt kinase can represent a functional link between insulin resistance and inflammation, because it phosphorylates and thereby activates IκB kinase, which further activates the NF-κB signaling pathway (36). Also, cytokine-activated JNK can phosphorylate IRS-1 serine residues thus inhibiting insulin signaling and causing peripheral insulin resistance (37).

Fructose-induced disturbances in brain insulin signaling can lead to dysfunction of neurons and disorders of cognitive functions (38, 39). Fructose feeding was previously reported to induce insulin signaling impairment (40, 41), reduce neurogenesis (42), elicit neuroinflammation (43) and negatively impact brain plasticity in rat hippocampus (44) and frontal cortex (45). Since the majority of fructose effects in the brain were investigated in hippocampus, the present study is focused on prefrontal cortex, and what is more important, it has been demonstrated that high-fat and sugar diets induce severe frontal-dependent cognitive deficits (46–48). Studies on hippocampus have pointed that the main mechanisms underlying impairments in spatial memory and learning in rodents is increase in neuroinflammatory markers (49), as well as alterations in hippocampal insulin signaling, IGF-1 and BDNF levels (50). The role of insulin signaling in the promotion of neuroplasticity in the adult brain has been recently documented (51). One of the proposed mechanisms is PKC-dependent, suggesting that the net effect of this kinase and its interaction with insulin appears to be induced synaptogenesis and stimulated neurorepair in adult brain (52). IGF-1 influences growth, proliferation, and maturation of neurons and glia, as well as the neuronal

myelinization (53). It promotes these effects through modulation of downstream kinases linked to inflammation, neurodevelopment, aging and synaptic function, among which is the calcium calmodulin dependent kinase 2 alpha (CaMKIIα) (54). Another trophic factor, BDNF plays an important role in improving the state of insulin resistance, maintaining glucose homeostasis and controlling food intake (55). Recent study indicated that cognitive decline of offspring from fructose-fed mothers is associated with suppressed *Bdnf* transcription through increased DNA methylation of the *Bdnf* promoter region (56). Besides trophic factors, very important factors for the regulation of cognitive and other complex functions in the frontal cortex are pre-synaptic proteins, such as synaptophysin, involved in the regulation of the kinetics of synaptic vesicle endocytosis (Kwon and Chapman, 2011), and post-synaptic density (PSD-95) proteins, pivotal for the protein scaffolding in excitatory neurons (57).

Taking into account that fructose diet can affect brain insulin sensitivity and plasticity through changes in inflammation, the aim of this study was to examine the underlying role of pro-inflammatory cytokine MIF in inflammation, insulin sensitivity and plasticity of the PFC in male mice fed with high fructose diet.

2. Experimental Procedures

2.1. Animals and treatment

The generation of homozygous *Mif* gene-deficient (MIF-KO) mice on C57BL/6J background has been described previously (58). Breeder mice (MIF-KO and WT) were a kind gift from Dr. Christine Metz (Laboratory of Medicinal Biochemistry, The Feinstein

Institute for Medical Research, NY) to Dr. Stanislava Stosic Grujicic from the Institute for Biological Research "Siniša Stanković". All animals were bred under standard pathogen-free laboratory conditions in the Animal Facility of the Institute. During nine weeks, 4 animals per cage were kept in a temperature-controlled room (22 ± 2°C) with a 12h light/dark cycle (lights on at 07:00 h). The 2 months old male mice were divided into 4 experimental groups (n = 8 animals per group): WT and MIF-KO mice had standard diet commercial chow (Veterinary Institute, Subotica, Serbia) and drinking water available *ad libitum*. WT and MIF-KO mice on fructose rich diet (WT+F and MIF-KO+F) had *ad libitum* access to commercial chow and to 20% fructose (API-PEK, Bečej, Serbia) solution instead of drinking water. The concentration of fructose solution was chosen to induce metabolic disturbances (9, 59). The detailed composition of the diet was described previously (60). All animal procedures were in compliance with the EEC Directive 2010/63/EU on the protection of animals used for experimental and other scientific purposes, and were approved by the Ethical Committee for the Use of Laboratory Animals of the Institute for Biological Research "Siniša Stanković", University of Belgrade (No. 03-12/15).

2.2. Behavioral testing

During the last five days of the treatment, all mice were submitted to elevated plus maze (EPM), light-dark box (LDB) and novel object recognition (NOR) test (days: -1, -3, -5, between 9 AM and 1 PM). The tests were performed at 25ºC, in a dimly illuminated room (indirect 2 x 40 W light) with light and acoustic isolation. Videos of mouse activities were registered by the camera connected to a PC and analyzed by ANY-maze Video Tracking

System 4.30 (Stoelting Co., USA). Particular behavioral parameters were identified and counted by a proficient experimenter, who was unaware of the experimental groups. After each test, the equipment was cleaned with 10% ethanol solution and dried with paper towels, to remove any trace of odor.

For the EPM test, mouse movements were recorded for 5 min by a video camera mounted vertically above the apparatus, a cross-shaped Plexiglas platform elevated 50 cm from the floor. This apparatus consisted of two opposite open arms (OA, 50 × 10 cm), and two opposite closed arms (CA, 50 × 10 cm) with 40 cm walls, connected by a central platform (CP, 10 × 10 cm), where each animal was placed at the start of a test. The level of a mouse anxiety was estimated by the number of entries into OA (presented as % of total entries) and by latency to first entrance into OA.

LDB was made from Plexiglas (50 cm × 25 cm × 30 cm (H)) and divided into one-third, covered and dark compartment, while the rest of the box was open and alight. The barrier had a loose door that allowed free transitions between the compartments. The 5 min test sessions were video registered after each mouse had been placed in the middle of the illuminated compartment and allowed to move freely. Their time spent in the dark vs. light compartment and the latency to first enter into dark compartment were measured and compared among the groups.

The variant of NOR applied in our experiments was adapted from the published procedure by Hammond et al. (61). Each animal was allowed a 10 min training session with the exposure to two identical, non-toxic objects (hard plastic item) placed in the two opposite corners of the arena (45x45 cm). After the training session, animal was returned to its home

cage for a 30-min retention interval, before it was submitted to the test, in which one familiar object was replaced with a novel object of a similar size, but with different shape. The animal was placed into the arena, equidistant and facing away from both objects. The exploration was defined when the animal's head was inside a circle (R=6 cm) around the object. Each mouse was excluded from further exploratory registration after accumulating 40 s of exploration time on either of the sample objects. The novel object preference ratios (in % of time) were calculated by dividing the novel object exploratory time with the time used to explore both objects (40 s). A value above 50% suggests preference for the novel object, while a value below 50% is indicative of familiar object preference.

2.3. Parameters of systemic insulin sensitivity

In order to determine insulin sensitivity, the homeostatic model assessment of insulin resistance (HOMA-IR) index, quantitative insulin sensitivity check index (QUICKI) and revised quantitative insulin sensitivity check index (R-QUICKI) were determined. HOMA index was calculated from fasting plasma insulin and glucose concentrations using the following formula: insulin (mU/l) × glucose (mmol/l)/22.5.QUICKI and R-QUICKI were calculated using formulas 1/[log insulin (μU/mL) + log glucose (mg/dL)] and 1/[log insulin (μU/mL) + log glucose (mg/dL) + log NEFA (mmol/l)], respectively.

2.4. RNA extraction and Reverse Transcription

Animals were killed by rapid decapitation and the prefrontal cortices were carefully

excised and immediately frozen and kept in liquid nitrogen until use.

Total RNA was isolated using TRIzol® (AmBion, Life Technologies, Carlsbad, USA). After homogenization, samples were centrifuged at 12000 g for 15 min at 4°C. RNA was precipitated with isopropanol. Quantitative evaluation of the isolated RNA was performed spectrophotometrically (OD 260/280 > 1.8 was considered satisfactory) and its quality was confirmed on 2% agarose gel. Reverse transcription was performed using a High-Capacity cDNA Reverse Transcription Kit (Applied Biosystems, Foster City, USA) according to the manufacturer's instructions and the cDNAs were stored at -70°C until use.

2.5. Real-time PCR

The expression of genes was analyzed using Power SYBR® Green PCR Master Mix. Specific primers (Applied Biosystems, Foster City, USA) were used to selectively amplify *Igf-1*: F: 5'-AGA CAG GCA TTG TGG ATG AG-3', R: 5'-TGA GTC TTG GGC ATG TCA GT-3'; *Tnf-α*: F: 5'-TCG AGT GAC AAG CCC GTA GC-3', R: 5'-CTC AGC CAC TCC AGC TGC TC-3'; *Bdnf-9*: F: 5'-TGC AGG GGC ATA GAC AAA AG-3', R: 5'-TGA ATC GCC AGC CAA TTC TC-3'; *Il-1β*:F: 5'-CAC CTC TCA AGC AGA GCA CAG-3', R: 5'-GGG TTC CAT GGT GAA GTC AAC-3'; *Tlr-4*: F: 5'-ATC ATC CAG GAA GGC TTC CA-3', R: 5'-GCT AAG AAG GCG ATA CAA TTC-3';*MyD88*: F: 5'-TCA TGT TCT CCA TAC CCT TGGT-3', R: 5'- GAC TGG GGT GAG CGT CAA A-3'; *Arg-1*: F: 5'-TAACCTTGGCTTGCTTCGG-3', R: 5'- GTGGCGCATTCACAGTCAC-3'; *Lif*: F: 5'-CCCTGAAGACTGGACAACTGTG-3', R: 5'- CAGAACCAGCAGCAGTAAGGG-3'; *Mrc-1*: F: 5'-GTTGTATTCTTTGCCTTTCCCAG-3', R: 5'-

CGTCTGAACTGAGATGGCACT-3'. Normalization of cDNA in each sample was performed using hypoxanthine guanine phosphoribosyl transferase (*Hprt*) as the endogenous control (F: 5'-TCC TCC TCA GAC CGC TTT T-3', R: 5'-CCT GGT TCA TCA TCG CTA ATC-3'). All reactions were performed in triplicate in 25 µl volume containing 20 ng of cDNA template using Quant Studio™ 3 (Applied Biosystems, Foster City, USA). Thermal cycling conditions were 2 min incubation at 50 °C, 10 min at 95 °C followed by 60 cycles of 95 °C for 15 s and 60 °C for 60 s. Melting curve analyses were performed at the end of every experiment to confirm formation of a single PCR product. Relative quantification of gene expression was performed using the comparative $2^{-\Delta\Delta Ct}$ method. The results were analyzed by Quant Studio™ Design and Analysis Software v1.4.0 (Applied Biosystems, Foster City, USA) with a confidence level of 95% ($p \leq 0.05$).

2.6. Preparation of total protein

For the preparation of total protein fraction, the remaining organic phase (obtained after aqueous phase separation for RNA precipitation) was centrifuged at 2000 g for 5 min at 4°Cafter adding ethanol. Protein fraction was precipitated from phenol-ethanol supernatant, using acetone and centrifuged at 12000 g for 10 min at 4°C. The protein pellets were dispersed in 0.3 M guanidine hydrochloride in 95% ethanol with 2.5% glycerol by sonication on ice and washed in 0.3 M guanidine hydrochloride in 95% ethanol with 2.5% glycerol. After sedimenting the protein by centrifugation at 8000 g for 5 min at 4°C, pellets were dispersed in the lysis buffer containing 2.5 mM Tris-HCl pH 6.8, 2% SDS, 10% glycerol and 50 mM DTT. All samples were stored at −70°C.

2.7. Western blot analysis

The samples were mixed with denaturing buffer, boiled, and 40 µg of proteins were subjected to 10% (pAkt 1/2/3 Ser473,Akt 1/2/3, AMPKα1/2 and pAMPKαThr 172, 11β-HSD1, GR, pGR Ser 220, syntaptophysin, F4/80, NF-κB, IκB, pIκB Ser32) or 7.5% (IRβ, pIRS-1 Ser307, pIRS-1 Ser1101IRS-1, PSD-95, PKCα, pPKCα-Ser657, CaMKIIα, pCaMKIIα-Thr286, GSK-3β, pGSK-3β Ser9) SDS-PAGE. After electrophoresis, proteins were transferred onto PVDF membrane (Immobilon-P, Millipore, USA) using a blot system (Transblot, BioRad, USA). Membranes were blocked for 1 h with 5% non-fat dry milk dissolved in phosphate buffered saline (PBS) at room temperature and incubated with the respective primary and secondary antibodies: anti-phospho-IRS-1 Ser 307 (sc-33956, 1:1000); anti-IRS-1 (sc-8038, 1:250); anti-phospho-Akt 1/2/3 (Ser473, sc-7985-R, 1:2000); anti-Akt 1/2/3 (sc-8312, 1:2000); anti-AMPKα1/2 (sc-25792, 1:1000); anti-GR (sc-8992, 1:250); anti-NFκB/p65 (C-20) (sc-372, 1:000); anti-IκB-α (C-21) (sc-371, 1:500); anti-F4/80 (M-17)-R (sc-26643-R, 1:500); anti-insulin Rβ (C-19) (sc-711, 1:500); anti-pPKCα-Ser657 (sc-12356, 1:500); anti-PKCα (H-7) (sc-8393, 1:500); anti-pCaMKIIα-Thr286 (sc-12886-R, 1:10000); anti-CaMKII (M-176) (sc-9035, 1:10000); anti-GSK-3α/β (0011-A) (sc-7291, 1:1000) and anti-pGSK-3β (F-2) (sc-373800, 1:1000) were from Santa Cruz Biotechnology (Dallas, Texas, USA), while anti-phospho-IRS1-Ser 1101 (#2385, 1:500); anti-PSD95 (#2507, 1:1000); anti-phospho-IκBα (Ser32) (14D4) (#2859, 1:500); anti-pAMPKα Thr 172 (#2535s, 1:1000) and anti-pGR Ser 211/220/232 (#4161S, 1:1000) were obtained from Cell Signaling Technology (Danvers, Massachusetts, USA). Anti-synaptophysin (SP11): MA5-

14532 (1:1000) was from Invitrogen (Waltham, Massachusetts, USA).Anti-11β-HSD1 (ab39364, 1:1000), as well as anti-β-actin (ab8227, 1:10000), used as a loading control, were both from Abcam (Cambridge, UK). Blots were developed with ECL Anti-Rabbit IgG, HRP-linked whole antibody ab6721 (Abcam) or with Anti-Mouse IgG H&L (HRP) ab97046 (Abcam). Densitometry of protein bands was detected using iBright FL1500 Imaging System (Thermo Fisher Scientific, MA, USA).

2.8. Statistical analyses

Data are presented as mean ± SEM. The data were tested for normality by the Kolmogorov-Smirnov test. Normally distributed data were analyzed by one-way ANOVA followed by Tukey *post-hoc* test. A p value < 0.05 was considered statistically significant. Statistical analyses were performed by using GraphPad Prism v5 Software (USA).

3. Results

3.1. Markers of inflammation in the prefrontal cortex

Inflammation in the PFC was estimated through NF-κB signaling pathway, the expression of genes for pro-inflammatory cytokines IL-1β and TNF-α, as well through gene expression of *Tlr-4* and *MyD88*. In addition, the activation of microglia was assessed at the protein level of F4/80 and mRNA level of *Arg-1*, *Lif* and *Mrc-1*. There was no statistically significant changes between the investigated groups in the expression of *Il-1β* (Table 1) and protein levels of F4/80, NF-κB/p65 subunit and IκB and its phosphorylation (Figure 1B and C). However, significant differences were observed in one-way ANOVA for mRNA levels

of *Tnf-α* (Table 1, F=6.10, p<0.01), *Tlr-4* (Table 1, F=117.10, p<0.001), *MyD88* (Table 1, F=436.70, p<0.001), *Arg-1* (Figure 1D, F=803.60, p<0.001), *Lif* (Figure 1D, F=15.10, p<0.001) and *Mrc-1* (Figure 1D, F=19.99, p<0.001). Post-hoc Tukey test showed significant increase in the relative mRNA level of *Tnf-α* (*p<0.05), *Lif* (**p<0.01) and *Tlr-4*, *MyD88*, *Arg-1*and *Mrc-1* (***p<0.001) in the PFC of MIF-KO mice on standard diet when compared to the WT. In the case of *Arg-1*, significant downregulation was also observed in MIF-KO animals on fructose diet in comparison to the standard-fed WT (***p<0.001). Also, the analysis confirmed a significant reduction of *Tnf-α* ($^{\#}$p<0.05), as well as the reduction of *Tlr-4*, *MyD88*, *Arg-1*, *Lif* and *Mrc-1* ($^{\#\#\#}$p<0.001) mRNA levels in the PFC of fructose-fed MIF-KO mice compared to standard-fed MIF-KO animals.

3.2. Markers of insulin sensitivity and energy balance

Systemic insulin sensitivity was assessed at the level of HOMA-IR index and QUICKI and R-QUICKI. One-way ANOVA confirmed significant differences for all analyzed parameters, HOMA-IR (F=5.78, p<0.01), QUICKI (F=14.12, p<0.001) and R-QUICKI (F=14.53, p<0.001). As shown in Table 2, post-hoc test showed that HOMA-IR was significantly higher in fructose-fed MIF-KO mice compared to the wild type animals (**p<0.01, MIF-KO + F vs. WT), while QUICKI and R-QUICKI were significantly decreased in both MIF-KO groups regardless of the diet (***<0.001, MIF-KO vs. WT and MIF-KO + F vs. WT). In addition, HOMA-IR was higher (††p<0.01), while QUICKI and R-QUICKI were lower (†††p<0.001) in fructose-fed MIF-KO mice in comparison to the WT animals on the same diet.

In order to assess insulin sensitivity in the PFC, protein levels of IR and IRS-1 were analyzed together with IRS-1 inhibitory phosphorylations at serine 307 and serine 1101. As shown in Figure 2, IRS-1 signaling remained unchanged in the PFC of all experimental groups. However, one-way ANOVA revealed significant differences for IR protein level ($F=28.49$, $p<0.001$) and IRS-1 serine 1101 phosphorylation ($F = 5.049$, $p<0.001$). Post-hoc test confirmed significant decrease of IR protein level in all experimental groups in comparison to the wild type animals on standard diet (**p<0.01, MIF-KO vs. WT; ***p<0.001, MIF-KO + F vs. WT, WT + F vs. WT), while IR protein level was significantly higher in fructose-fed MIF-KO mice in comparison to the wild type animals on the same diet (†p<0.05, MIF-KO + F vs. WT + F). Also, IRS-1 serine 1101 phosphorylation was significantly higher in fructose-fed MIF-KO mice in comparison to wild type animals on both standard and fructose diet (*p<0.05, MIF-KO vs. WT; †p<0.05, MIF-KO + F vs. WT + F).

Also, protein levels of PKCα, Akt, GSK-3β and AMPK were analyzed, together with their phosphorylations and ratios of phosphorylated to total protein levels (Figure 3). One-way ANOVA showed significant differences for PKCα protein level ($F=11.77$, $p<0.001$), its phosphorylation at serine 657 ($F=15.13$, $p<0.001$) and pPKCα/PKCα ratio ($F=5.25$, $p<0.01$). Post-hoc test revealed significant decrease of pPKCα in all experimental groups in comparison to the wild type animals on standard diet (Figure 3A, ***p<0.001, MIF-KO vs. WT, MIF-KO + F vs. WT, WT + F vs. WT), while PKCα protein level was significantly decreased in standard-fed MIF-KO mice and fructose-fed WT mice in comparison to the wild type animals (***p<0.001, MIF-KO vs. WT and **p<0.01, WT + F vs. WT). Also total PKCα protein level was significantly higher in fructose-fed MIF-KO mice when compared

to the MIF-KO mice on standard diet ($^{\#\#}p<0.01$). Finally, in the case of pPKCα/PKCα ratio, fructose-fed MIF-KO mice exhibited lower ratio than standard-fed WT (*p<0.05, MIF-KO + F vs. WT) and MIF-KO ($^{\#\#}p<0.01$, MIF-KO + F vs. MIF-KO) animals. One-way ANOVA revealed significant differences for Akt protein level ($F=5.21$, $p<0.01$) and pAkt/Akt ratio ($F=8.37$, $p<0.001$). Post-hoc test confirmed significant decrease of Akt protein level in all experimental groups in comparison to the wild type animals on standard diet (Figure 3B, *p<0.05, MIF-KO vs. WT, MIF-KO + F vs. WT, WT + F vs. WT), while pAkt/Akt ratio was significantly increased in standard-fed MIF-KO mice and fructose-fed WT mice in comparison to the wild type animals (**p<0.01, MIF-KO vs. WT and WT + F vs. WT). As shown in Figure 3C, there was no change at the protein level and phosphorylation of the GSK-3β. Ratio of phosphorylated AMPKα at Thr172 to total AMPKα protein level was used as a marker of energy balance. One-way ANOVA did not reveal significant differences in total AMPKα protein level, while these differences were statistically significant for pAMPKαThr172 ($F=7.99$, $p<0.001$) and for pAMPKα/AMPKα ratio ($F=12.90$, $p<0.001$). As shown in Figure 3D, post-hoc test revealed significant reduction in the PFC of mice from all experimental groups in comparison to the wild type mice on standard diet in both pAMPKαThr172 (**p<0.01, MIF-KO vs. WT, MIF-KO + F vs. WT and *p < 0.05, WT + F vs. WT) and pAMPKα/AMPKα ratio (***p<0.001, MIF-KO vs. WT, MIF-KO + F vs. WT and WT + F vs. WT).

3.3. Glucocorticoid signaling in the prefrontal cortex

Glucocorticoid signaling was examined at the protein level of 11β-HSD1 enzyme of the prereceptor metabolism, as well as at the level of total GR, its activating serine 220 phosphorylation and their ratio. One-way ANOVA revealed significant differences for pGR ($F=3.13$, $p<0.05$) and pGR/GR ratio ($F=9.86$, $p<0.001$), post-hoc test did not show significant inter-group differences for 11β-HSD1 and both pGR and GR protein levels (Figure 4). However, pGR/GR ratio was markedly higher in the PFC of fructose-fed WT mice compared to the standard-fed WT (**$p<0.01$, WT + F vs. WT), which was abolished in MIF-KO animals on fructose diet ($^{\dagger\dagger}p<0.01$, MIF-KO + F vs. WT + F).

3.4. Markers of neural plasticity in the prefrontal cortex

Plasticity of the PFC was assessed at the phosphorylation level of CaMKII, protein level of PSD-95 and synaptophysin, and at the mRNA level of BDNF-9 and IGF-1. One-way ANOVA showed significant differences for CaMKII ($F=59.29$, $p<0.001$), its threonine 286 phosphorylation ($F=84.25$, $p<0.001$) and their ratio ($F=94.72$, $p<0.001$), as well as for the PSD-95 protein level ($F=18.64$, $P<0.001$) and the relative mRNA level of BDNF-9 ($F=196.60$, $p<0.001$) and IGF-1 ($F=59.29$, $p<0.001$). As shown in Figure 5A, significant increase of CaMKII phosphorylation was observable in all experimental groups in comparison to the wild type animals on standard diet (Figure 5B, ***$p<0.001$, MIF-KO vs. WT, MIF-KO + F vs. WT, WT + F vs. WT), while this phosphorylation was significantly lower in MIF-KO + F group in comparison to the WT mice on fructose diet ($^{\dagger\dagger\dagger}p<0.001$). Total CaMKII protein level was increased in both fructose-fed groups (**$p<0.01$, MIF-KO + F vs. WT, ***$p<0.001$, WT + F vs. WT). Finally, pCaMKII/CaMKII ratio was also significantly increased in all experimental groups in comparison to the wild type animals on

standard diet (Figure 5B, ***p<0.001, MIF-KO vs. WT, MIF-KO + F vs. WT, WT + F vs. WT), while the ratio was lower in fructose-fed MIF-KO mice when compared to both WT mice on fructose diet (†††p<0.001) and to standard-fed MIF-KO mice ($^{\#}$p<0.05, MIF-KO + F vs. MIF-KO). Additionally, protein level of PSD-95 was significantly lower in standard-fed MIF-KO mice in comparison to the WT animals on the same diet (Figure 5C, ***p<0.001), while in fructose-fed MIF-KO mice it raised back to the control level ($^{\#\#}$p<0.01). As shown in Figure 5D, post-hoc analysis showed significant increase in the relative level of BDNF-9 and IGF-1 mRNA in standard-fed MIF-KO mice in comparison to the WT (***p<0.001). In addition, a significant decrease in mRNA levels for both BDNF-9 and IGF-1 was detected in fructose-fed MIF-KO mice when compared to the same animals on standard diet ($^{\#\#\#}$p<0.001).

3.5. Behavioral tests

One-way ANOVA showed that latency to enter OA was significantly affected (F=2.85, *p<0.05), while the % of total crossings into open arms of the EPM was not changed. Post-hoc test revealed that MIF-KO mice on standard diet exhibit higher latency to enter the OA, in comparison to the WT animals on the same diet (Fig. 6A, *p<0.05). Preference of mice for the dark box, expressed by the increased time spent in this compartment and the reduction of latency for the first entrance into the dark part (Fig. 6C and D), were significantly affected (F=3.89, p<0.05 and F=7.95, p<0.01). Post hoc test revealed that standard-fed *Mif* deficient mice had reduced latency to enter dark compartment (*p<0.05) and spent more time in dark then WT animals (**p<0.01), while fructose diet led

to reduction of this time ($^{\#}p<0.05$). Novel object preference ratio (expressed in %) was significantly affected ($F=4.06$, $p<0.05$). Post hoc test revealed that this behavioral parameter was significantly lower in standard-fed MIF-KO mice (Figure 6E, $^{*}p<0.05$) in comparison to the standard-fed WT mice.

4. Discussion

The aim of the study was to examine the role of *Mif* in the local inflammation in the PFC, as well as its possible link to insulin resistance, plasticity and behavioral impairments under the conditions of energy overload induced by fructose overconsumption. The results showed increased mRNA level of pro-inflammatory mediators in conjunction with increased markers of M2 microglial activation (*Arg-1*, *Mrc-1*) in the PFC of MIF-KO animals on standard diet. This was paralleled with significantly increased trophic factors BDNF-9 and IGF-1 on the one side, and decreased PSD-95 protein level and impaired behavior on another. Insulin signaling was not disturbed in the PFC of MIF-KO animals, as seen on increased pAkt/Akt ratio and unchanged PKCα and GSK-3 activity. Fructose feeding of the MIF-KO mice restored these parameters in the PFC to the control level and mitigated behavioral changes.

It was previously demonstrated that *Mif* deficient mice exert strong anti-inflammatory phenotype (12) and higher levels of anti-inflammatory cytokines in cardiac tissue (13). It has also been reported that *Mif* deficiency may down-regulate TLR-4 expression in macrophages (11). In this study, we found significantly increased *Tnf-α*, *Tlr-4* and *MyD88* mRNA levels in the PFC of MIF-KO mice. This finding could point to the possible existence of a

compensatory mechanism for *Mif* deficiency in the brain, as seen previously for the compensatory enhanced production of TNF-α in the IL1-KO mice (62). Alternative explanation for increased *Tlr-4* and *MyD88* in the absence of MIF could be found in the elevation of circulatory endotoxins due to the disrupted intestinal barrier permeability and altered diversity and content of gut microbiota in MIF-KO mice, which is known to activateTLR-4/MyD88 complex (63). This increase in proinflammatory mediators was not accompanied with increased expression and activity of NF-κB, which implies that some other transcriptional regulators, such as AP1 or JNK, could be responsible for the observed effects. It cannot be neglected as well that these pro-inflammatory mediators were analyzed at the transcriptional level, and that posttranslational modifications can also modify their activity. Nevertheless, in accordance with the applied methods, we suggest that *Mif* deficiency in the PFC leads to transactivation of genes for pro-inflammatory mediators. Since F4/80 protein, which is the marker of peripheral macrophages and resting microglia, was not changed between the experimental groups, we presume that the increased transcription of proinflammatory mediators is linked to the activation of proinflammatory M1 microglia in the PFC. Interestingly, the markers of alternative anti-inflammatory M2 microglia, *Arg-1* and *Mrc-1*, were also increased in MIF-KO group, implying the concurrent activation of M1 and M2 microglia in the state of *Mif* deficiency. Indeed, there are studies showing mixed M1 and M2 microglia phenotype with concomitant expression of both pro- and anti-inflammatory genes (64, 65). Although it became clear that individual cells can express transitional phenotypes, it is still not certain whether M1 and M2 are phenotypically distinct subpopulations of microglia that perform different functions within different stages of

inflammatory response, or whether they shift between functional phenotypes depending on environmental signals (66). Nevertheless, it has been shown that transition from the M1 to the M2 phenotype promotes positive outcomes, since it facilitates resolution of inflammation through anti-inflammatory factors (such as *Arg-1* and *Mrc-1*), leading to deactivation of the proinflammatory cell phenotypes and re-establishment of homeostasis (67). Taking this into account, the observed presence of both M1 and M2 markers in our study could most likely be a part of the brain protective response to increased inflammation which aims to reduce the neuroinflammation-associated damage (64). This is also in accordance with the increased expression of *Lif*, previously shown to direct polarization microglia from pro-inflammatory towards anti-inflammatory phenotype (27). In addition, observed increase of M2 microglial markers goes in line with the increased level of neurotrophic factors, especially IGF-1. Namely, previous studies showed that M2-like macrophages are an important source of IGF-1 (68), and that specifically M2 microglia can enhance IGF-1 release to resolve inflammation and promote neuron survival (69).

Taking into account that excessive inflammation is usually associated with insulin resistance, we examined the key components of the PFC insulin signaling pathway, IR, IRS-1, and Akt, and specifically their phosphorylation-regulated activity, as well as the parameters of systemic insulin sensitivity (HOMA-IR, QUICKI and R-QUICKI). Among analyzed, total IR protein was decreased, both total IRS-1 and its inhibitory phosphorylations (at Ser307 and Ser1101) were unchanged, and protein level of total Akt was decreased in the PFC of MIF-KO mice. The latter is probably a consequence of increased TNF-α expression, since TNF-α was previously shown to be capable of inducing caspase-dependent degradation

of Akt (70). However, the pAkt/Akt ratio, taken as a marker of stimulated insulin signaling, was increased in the same animals, implying enhanced insulin signaling in the PFC of MIF-KO animals. This is in conjunction with unchanged phosphorylation of PKCα and GSK-3β, which implies that insulin signaling in the PFC was not disturbed due to *Mif* deficiency. The finding that MIF-KO mice exhibited signs of disturbed systemic insulin sensitivity, as judged by increased HOMA-IR, and decreased QUICKI and R-QUICKI, together with previously observed hyperglycemia, hyperinsulinemia and impaired glucose and insulin tolerance in the same animals (9) seems discordant to the increased Akt activation observed in the PFC of MIF-KO mice. However, it has been previously demonstrated that brain Akt kinases could be hyperactivated in the insulin-resistant *ob*/*ob* mice on high-fat diet (71). The observed discordance is most likely the result of the phenomenon of selective insulin resistance in the CNS, which can result in the inhibition of insulin signaling pathways in some tissues and even brain regions, and over activation in others (72). Indeed, we have previously shown signs of insulin resistance in the hippocampus of these animals (73). The observed increase in pAkt/tAkt ratio is also in accordance with increased *Igf-1* mRNA levels demonstrated in the MIF-KO animals, since it is known that IGF-1 receptor activation triggers the PI3K-Akt signaling pathway (74). Finally, it is noteworthy that IGF-1/Akt signaling was shown to be associated with enhanced ability of macrophages to transform to the M2 state (75).

Since inflammation in the brain can lead to pathophysiological changes, further investigation of neurotrophic factors in the PFC was performed. Expression of both *Bdnf-9* and *Igf-1* was significantly increased in the MIF-KO mice, which could be ascribed to M2 microglial activation as a part of the protective mechanism against neuroinflammation-

associated damage (69). Previous studies suggest that an increase in neural plasticity could counterbalance activation of the immune response, thus keeping inflammation in a limited range (76). However, there are several steps between mRNA and mature protein, which in case of BDNF include the formation of apoptosis-inducing pro-BDNF (77), while in this study only mRNA levels of these factors were assessed. In the present study, *Mif* deficient mice exhibited anxiogenic-like behavior, reflected in increased latency to enter the OA in the EPM and prolonged time spent in the dark compartment of the DLB. Additionally, impairment in learning and memory in MIF-KO mice was also confirmed by the lower novel object preference ratio. These behavioral changes were accompanied with the lower level of PSD-95 observed in the PFC, which is accordance with previous finding that PSD-95 deficiency disrupts PFC-associated function and behavior, particularly learning and working memory (78). We also propose that the observed anxiogenic-like behavior in *Mif* deficient mice could be PSD-95 dependent, since dysfunction of PSD-95 is known to induce anxiety-like behavior (79). Taking into account that PSD-95 synthesis is modulated by inflammation (80), whereas increase in TNF-α leads to its reduction (81), we presume that increased inflammation in *Mif* deficient mice represents primary event leading to downregulation of PSD-95 and associated cognitive and mood impairments. Thus, it could be proposed that behavioral deteriorations are most likely a consequence of enhanced inflammation and downregulation of PSD-95, while elevation of neurotrophic factors may represent an accompanying compensatory mechanism. This compensatory mechanism involves increase of IGF-1, BDNF and CaMKII, the latter representing downstream target of IFG-1 (82), while synaptophysin, the other IFG-1 regulated protein, was not changed. However, when MIF-

KO mice were given fructose-enriched diet, it annulled the effects of *Mif* deficiency on examined neurotrophic factors as well as on PSD-95 and returned them to the control level, which was followed with amelioration of behavioral changes.

When applied alone in the present study, fructose-enriched diet did not change the level of pro-inflammatory mediators and kinases, nor affected the expression of M2 microglial markers. This was accompanied with unchanged expression of neurotrophic factors, PDS-95 and synaptophysin, which overall indicates that fructose diet did not affect neuronal plasticity and consequently behavior, as compared to WT animals on standard diet. On the other hand, the effects of fructose on insulin signaling were similar to the ones observed for standard-fed *Mif* deficient mice, e.g. decreased level of total IR, unchanged PKCα, and increased activation of Akt kinase, without concomitant change of IRS-1 and its phosphorylations at Ser307, while increased phosphorylation of IRS-1 at Ser1101 was observed. This phosphorylation, identified as S6K1 site in IRS-1, was found to be increased upon nutrient overload (83). However, its ratio to total IRS-1 protein level remained unchanged in the PFC of fructose-fed MIF-KO mice. In addition, in the same animals, reduced expression of *Tlr-4*, *Tnf-α* and *MyD88* was observed. This result was very intriguing, since fructose has considered to be proinflammatory in many tissues as recently thoroughly reviewed in Spagnuolo et al. (84). Such effect of fructose has also been reported for different brain regions (7, 40, 84), where it is promoted through TLR4/NF-κB signaling pathway (85). To our knowledge, there are no other inflammatory states in which fructose exhibits direct anti-inflammatory effect. However, much of the recent attention has been focused on neuroprotective action of fructose 1,6-bisphosphate (FBP), a high-energy intermediate of

fructose metabolism (86). It has recently been confirmed that many brain regions express fructose transporters and can metabolize fructose (87), which points to the importance of fructose metabolites for different brain functions. Specifically, FBP acts through anti-inflammatory and immunomodulatory mechanisms (86, 88), and has been shown to suppress MyD88-dependent signaling pathway (89), which was increased in the PFC of MIF-KO mice in our study. The immunosuppressive effects of fructose could also be indirect, and possibly mediated through glucocorticoids, potent anti-inflammatory hormones. Namely, we have previously shown that both glucocorticoid prereceptor metabolism and GR were upregulated by fructose in the hippocampus of rats drinking 60% fructose solution, opposing the action of NF-κB, and resulting in the unchanged expression of proinflammatory cytokines (90). Nevertheless, the results did not reveal any change at the level of 11β-HSD1 and total GR, pointing that the observed immunosuppressive effect of fructose in the PFC of MIF-KO mice was independent of the glucocorticoid signaling. While we confirmed that fructose diet increases stimulatory phosphorylation of GR in the PFC of WT mice, this effect was missing in MIF-KO animals, implying that MIF presence is necessary for the activation of glucocorticoids (14). Finally, the signals that originate from peripheral organs, such as increased leptin from the adipose tissue (9), or increased circulatory corticosterone (due to *Mif* deficiency) (91), could also indirectly modulate the effects of fructose in the brain of MIF-KO animals. According to the results presented herein, and the fact that direct anti-inflammatory effects of fructose were not previously reported, it seems that the observed immunomodulatory effects of fructose could rather be related to MIF or to the environment created in the PFC by its genetic deletion.

The state of suppressed inflammation after fructose-enriched diet was in accordance with the restoration of BDNF-9 and IGF-1 mRNA levels in the PFC of fructose-fed MIF-KO mice, as well as with increased PSD-95 and normalization of analyzed behavioral changes. It was previously shown that sugar-rich diets can lead to decreased hippocampal BDNF mRNA levels in adult rats (92), and also in the offspring of fructose-fed dams, due to hypermethylation of *Bdnf* gene promoter (56). Similar effects of fructose consumption were also reported for IGF-1 mRNA levels in the rat liver (93), while IGF-1 receptor was decreased in the hypothalamus and hippocampus of fructose-fed rats (40). The molecular markers of insulin signaling, as well as AMPKα phosphorylation, where not changed in MIF-KO mice on fructose diet as compared to individual factors, with the exception of PKCα. These results generally suggest that fructose has beneficial effects on disturbances induced by neuroinflammation in *Mif* deficient animals, such as behavioral impairments, most likely through increased synthesis of endocannabinoids (94) and dopamine (95), which has been shown to decrease depression-like and anxiety-like behaviors in laboratory models (96) and inhibit cytokine production and expression of adhesion molecules (97), respectively. Taking into account that it has been shown that brain inflammation is associated with a weakened reward system (98) and that cerebral cortex is a part of the reward system based on signaling via opioid and endocannabinoid receptors (99), there is a possibility that fructose achieves its role in MIF-KO mice through the hedonistic aspect of the sugar consumption. It could be suggested, but remains beyond the scope of this manuscript, that prefrontal cortex and other structures of the corticolimbic pathway, responsible for reward-associated feeding behavior (100, 101), could have more significant role in response to fructose feeding, compared to

other brain regions. Indeed, our previous study already showed brain-region related differences in response to *Mif* deletion, since (contrary to the PFC) signs of insulin resistance and unchanged plasticity in the hippocampus of MIF-KO mice were observed (73).

Although the influence of dietary sugars on metabolic disorders is an expanding field of research, the studies regarding the role of specific brain structures, such as PFC, in the pathophysiology of these disorders are still scarce. The results obtained in this study show that *Mif* deficiency provokes compensatory increase in local inflammation in the PFC by increasing the levels of TNF-α, TLR-4 and MyD88, whereas increase of BDNF-9 and IGF-1 could represent counterbalancing response to the increased inflammation due to activation of alternative M2 microglia. *Mif* deficiency also alters neural plasticity by decreasing PSD-95, which is accompanied by anxiety-like behavior and learning and memory impairment. Fructose itself did not affect inflammation or plasticity, but in the MIF-KO mice was clearly capable to restore behavioral impairments and ameliorate inflammation in the PFC, which was independent of glucocorticoid signaling activation. Although all MIF-KO animals showed disturbed insulin sensitivity at the systemic level, this was not mirrored in the disturbed insulin signaling in the PFC. Also, our results clearly demonstrate that the effects of fructose on neuroinflammation and behavior depend on the presence of MIF, as seen for the activation of GR, PKCα and CaMKII kinase, which postulates that their regulation in the setting of metabolic stress by caloric overload is mediated, at least indirectly, through MIF.

Acknowledgements: The authors are thankful to Dr. Stanislava Stošić Grujičić and Dr. Ivana Stojanović for provision of the experimental animals.We would like to thank Dr. Goran Korićanac from the "Vinča" Institute of Nuclear Sciences for the provision of antibodies. Also, the authors are thankful to the colleagues from the Institute for Biological Research "Siniša Stanković": Dr. Vesna Pešić and Dr. Ivana Bjelobaba (Department of Neurobiology), Dr. Svetlana Dinić (Department of Molecular Biology) and Dr. Sanja Mijatović (Department of Immunology) for the support in materials for the experiments. We would also like to thank Dr. Mirko Tomić from the Department of Biochemistry for the help in the analyses of behavioral data.

Conflict of interest: The authors declare that they have no conflict of interest.

Author contributions: MV: investigation, formal analyses, writing. VŠ: investigation, formal analyses. BB: formal analyses, writing – original draft preparation. LG: visualization, formal analyses. DI: visualization, formal analyses, writing – review and editing. SK: visualization, formal analyses, writing – review and editing. NV: conceptualization, writing – review and editing. AD: conceptualization, supervision, writing – review and editing. All authors: final approval of the submitted version.

Data Availability Statement: The data that support the findings of this study are available from the corresponding author upon reasonable request.

Funding: This work was supported by the Ministry of Education, Science and Technological Development of the Republic of Serbia under Grant No 451-03-9/2021-14/ 200007. The funders had no role in the design, analysis or writing of this article.

5. References

[1] Arnold, S. E., Arvanitakis, Z., Macauley-Rambach, S. L., Koenig, A. M., Wang, H. Y., et al. (2018) Brain insulin resistance in type 2 diabetes and Alzheimer disease: concepts and conundrums. *Nat Rev Neurol*. **14**, 168–181

[2] Greenwood, C. E., and Winocur, G. (2005) High-fat diets, insulin resistance and declining cognitive function. *Neurobiol Aging*. **26 Suppl 1**, 42–45

[3] de la Monte, S. M., and Wands, J. R. (2008) Alzheimer's disease is type 3 diabetes-evidence reviewed. *J Diabetes Sci Technol*. **2**, 1101–1113

[4] Berkowitz, R. L., Coplan, J. D., Reddy, D. P., and Gorman, J. M. (2007) The human dimension: how the prefrontal cortex modulates the subcortical fear response. *Rev Neurosci*. **18**, 191–207

[5] Nguyen, J. C., Killcross, A. S., and Jenkins, T. A. (2014) Obesity and cognitive decline: role of inflammation and vascular changes. *Front Neurosci*. **8**, 375

[6] Viollet, B., Horman, S., Leclerc, J., Lantier, L., Foretz, M., et al. (2010) AMPK inhibition in health and disease. *Crit Rev Biochem Mol Biol*. **45**, 276–295

[7] Zhang, D.-M., Jiao, R.-Q., and Kong, L.-D. (2017) High Dietary Fructose: Direct or Indirect Dangerous Factors Disturbing Tissue and Organ Functions. *Nutrients*. **9**, 335

[8] Cvetkovic, I., Al-Abed, Y., Miljkovic, D., Maksimovic-Ivanic, D., Roth, J., et al. (2005) Critical role of macrophage migration inhibitory factor activity in experimental autoimmune diabetes. *Endocrinology*. **146**, 2942–2951

[9] Gligorovska, L., Bursać, B., Kovačević, S., Veličković, N., Matić, G., et al. (2019) Mif deficiency promotes adiposity in fructose-fed mice. *J. Endocrinol.* 10.1530/JOE-

18-0333

[10] Lolis, E., and Bucala, R. (2003) Macrophage migration inhibitory factor. *Expert Opin Ther Targets*. **7**, 153–164

[11] Roger, T., Froidevaux, C., Martin, C., and Calandra, T. (2003) Macrophage migration inhibitory factor (MIF) regulates host responses to endotoxin through modulation of Toll-like receptor 4 (TLR4). *J Endotoxin Res*. **9**, 119–123

[12] Stojanovic, I., Cvjeticanin, T., Lazaroski, S., Stosic-Grujicic, S., and Miljkovic, D. (2009) Macrophage migration inhibitory factor stimulates interleukin-17 expression and production in lymph node cells. *Immunology*. **126**, 74–83

[13] Gao, X. M., Liu, Y., White, D., Su, Y., Drew, B. G., et al. (2011) Deletion of macrophage migration inhibitory factor protects the heart from severe ischemia-reperfusion injury: a predominant role of anti-inflammation. *J Mol Cell Cardiol*. **50**, 991–999

[14] Flaster, H., Bernhagen, J., Calandra, T., and Bucala, R. (2007) The macrophage migration inhibitory factor-glucocorticoid dyad: regulation of inflammation and immunity. *Mol Endocrinol*. **21**, 1267–1280

[15] Coutinho, A. E., and Chapman, K. E. (2011) The anti-inflammatory and immunosuppressive effects of glucocorticoids, recent developments and mechanistic insights. *Mol Cell Endocrinol*. **335**, 2–13

[16] Tomlinson, J. W., Walker, E. A., Bujalska, I. J., Draper, N., Lavery, G. G., et al. (2004) 11 beta-hydroxysteroid dehydrogenase type 1: A tissue-specific regulator of glucocorticoid response. *Endocr. Rev.* **25**, 831–866

[17] Rajapandi, T., Greene, L. E., and Eisenberg, E. (2000) The molecular chaperones Hsp90 and Hsc70 are both necessary and sufficient to activate hormone binding by glucocorticoid receptor. *J Biol Chem*. **275**, 22597–22604

[18] Webster, J. C., Jewell, C. M., Bodwell, J. E., Munck, A., Sar, M., et al. (1997) Mouse glucocorticoid receptor phosphorylation status influences multiple functions of the receptor protein. *J Biol Chem*. **272**, 9287–9293

[19] Bloom, J., and Al-Abed, Y. (2014) MIF: mood improving/inhibiting factor? *J Neuroinflammation*. **11**, 11

[20] Kielian, T., and Drewza, P. D. (2005) Cytokines and Brain. in *Inflammatory Disorders of the Nervous System* (Minagar, A. ed), Humana Press, 10.1385/1592599052

[21] Daneman, R., Zhou, L., Kebede, A. A., and Barres, B. A. (2010) Pericytes are required for blood-brain barrier integrity during embryogenesis. *Nature*. **468**, 562–566

[22] Boche, D., Perry, V. H., and Nicoll, J. A. (2013) Review: activation patterns of microglia and their identification in the human brain. *Neuropathol Appl Neurobiol*. **39**, 3–18

[23] Greter, M., Lelios, I., and Croxford, A. L. (2015) Microglia Versus Myeloid Cell Nomenclature during Brain Inflammation. *Front Immunol*. **6**, 249

[24] Gomes-Leal, W. (2019) Why microglia kill neurons after neural disorders? The friendly fire hypothesis. *Neural Regen Res*. **14**, 1499–1502

[25] Cherry, J. D., Olschowka, J. A., and O'Banion, M. K. (2014) Neuroinflammation

and M2 microglia: the good, the bad, and the inflamed. *J Neuroinflammation*. **11**, 98

[26] Zhang, L., Zhang, J., and You, Z. (2018) Switching of the Microglial Activation Phenotype Is a Possible Treatment for Depression Disorder. *Front Cell Neurosci*. **12**, 306

[27] Davis, S. M., Collier, L. A., Winford, E. D., Leonardo, C. C., Ajmo Jr., C. T., et al. (2018) Leukemia inhibitory factor modulates the peripheral immune response in a rat model of emergent large vessel occlusion. *J Neuroinflammation*. **15**, 288

[28] Borst, S. E. (2004) The role of TNF-alpha in insulin resistance. *Endocrine*. **23**, 177–182

[29] Lebovitz, H. E. (2001) Insulin resistance: definition and consequences. *Exp Clin Endocrinol Diabetes*. **109 Suppl**, S135-48

[30] Copps, K. D., and White, M. F. (2012) Regulation of insulin sensitivity by serine/threonine phosphorylation of insulin receptor substrate proteins IRS1 and IRS2. *Diabetologia*. **55**, 2565–2582

[31] Draznin, B. (2006) Molecular mechanisms of insulin resistance: serine phosphorylation of insulin receptor substrate-1 and increased expression of p85alpha: the two sides of a coin. *Diabetes*. **55**, 2392–2397

[32] Cross, D. A., Alessi, D. R., Cohen, P., Andjelkovich, M., and Hemmings, B. A. (1995) Inhibition of glycogen synthase kinase-3 by insulin mediated by protein kinase B. *Nature*. **378**, 785–789

[33] Mishra, D., and Dey, C. S. (2021) PKCalpha: Prospects in Regulating Insulin Resistance and AD. *Trends Endocrinol Metab*. **32**, 341–350

[34] Boucher, J., Kleinridders, A., and Kahn, C. R. (2014) Insulin receptor signaling in normal and insulin-resistant states. *Cold Spring Harb Perspect Biol*. 10.1101/cshperspect.a009191

[35] Zhang, Z., Liu, H., and Liu, J. (2019) Akt activation: A potential strategy to ameliorate insulin resistance. *Diabetes Res Clin Pr*. **156**, 107092

[36] Bai, D., Ueno, L., and Vogt, P. K. (2009) Akt-mediated regulation of NFkappaB and the essentialness of NFkappaB for the oncogenicity of PI3K and Akt. *Int J Cancer*. **125**, 2863–2870

[37] Solinas, G., and Becattini, B. (2017) JNK at the crossroad of obesity, insulin resistance, and cell stress response. *Mol Metab*. **6**, 174–184

[38] Gerozissis, K. (2008) Brain insulin, energy and glucose homeostasis; genes, environment and metabolic pathologies. *Eur J Pharmacol*. **585**, 38–49

[39] Cisternas, P., Salazar, P., Serrano, F. G., Montecinos-Oliva, C., Arredondo, S. B., et al. (2015) Fructose consumption reduces hippocampal synaptic plasticity underlying cognitive performance. *Biochim Biophys Acta*. **1852**, 2379–2390

[40] Yin, Q., Ma, Y., Hong, Y., Hou, X., Chen, J., et al. (2014) Lycopene attenuates insulin signaling deficits, oxidative stress, neuroinflammation, and cognitive impairment in fructose-drinking insulin resistant rats. *Neuropharmacology*. **86**, 389–396

[41] Cigliano, L., Spagnuolo, M. S., Crescenzo, R., Cancelliere, R., Iannotta, L., et al. (2018) Short-Term Fructose Feeding Induces Inflammation and Oxidative Stress in the Hippocampus of Young and Adult Rats. *Mol Neurobiol*. **55**, 2869–2883

[42] van der Borght, K., Kohnke, R., Goransson, N., Deierborg, T., Brundin, P., et al. (2011) Reduced neurogenesis in the rat hippocampus following high fructose consumption. *Regul Pept*. **167**, 26–30

[43] Li, J. M., Ge, C. X., Xu, M. X., Wang, W., Yu, R., et al. (2015) Betaine recovers hypothalamic neural injury by inhibiting astrogliosis and inflammation in fructose-fed rats. *Mol Nutr Food Res*. **59**, 189–202

[44] Jimenez-Maldonado, A., Ying, Z., Byun, H. R., and Gomez-Pinilla, F. (2018) Short-term fructose ingestion affects the brain independently from establishment of metabolic syndrome. *Biochim Biophys Acta Mol Basis Dis*. **1864**, 24–33

[45] Spagnuolo, M. S., Bergamo, P., Crescenzo, R., Iannotta, L., Treppiccione, L., et al. (2020) Brain Nrf2 pathway, autophagy, and synaptic function proteins are modulated by a short-term fructose feeding in young and adult rats. *Nutr Neurosci*. **23**, 309–320

[46] Reichelt, A. C., Killcross, S., Hambly, L. D., Morris, M. J., and Westbrook, R. F. (2015) Impact of adolescent sucrose access on cognitive control, recognition memory, and parvalbumin immunoreactivity. *Learn Mem*. **22**, 215–224

[47] Reichelt, A. C. (2016) Adolescent Maturational Transitions in the Prefrontal Cortex and Dopamine Signaling as a Risk Factor for the Development of Obesity and High Fat/High Sugar Diet Induced Cognitive Deficits. *Front Behav Neurosci*. **10**, 189

[48] Morin, J. P., Rodriguez-Duran, L. F., Guzman-Ramos, K., Perez-Cruz, C., Ferreira, G., et al. (2017) Palatable Hyper-Caloric Foods Impact on Neuronal Plasticity. *Front Behav Neurosci*. **11**, 19

[49] Hsu, T. M., Konanur, V. R., Taing, L., Usui, R., Kayser, B. D., et al. (2015) Effects

of sucrose and high fructose corn syrup consumption on spatial memory function and hippocampal neuroinflammation in adolescent rats. *Hippocampus*. **25**, 227–239

[50] Ross, A. P., Bruggeman, E. C., Kasumu, A. W., Mielke, J. G., and Parent, M. B. (2012) Non-alcoholic fatty liver disease impairs hippocampal-dependent memory in male rats. *Physiol Behav*. **106**, 133–141

[51] Ferrario, C. R., and Reagan, L. P. (2018) Insulin-mediated synaptic plasticity in the CNS: Anatomical, functional and temporal contexts. *Neuropharmacology*. **136**, 182–191

[52] Nelson, T. J., Sun, M. K., Hongpaisan, J., and Alkon, D. L. (2008) Insulin, PKC signaling pathways and synaptic remodeling during memory storage and neuronal repair. *Eur J Pharmacol*. **585**, 76–87

[53] Zheng, W. H., Kar, S., Dore, S., and Quirion, R. (2000) Insulin-like growth factor-1 (IGF-1): a neuroprotective trophic factor acting via the Akt kinase pathway. *J Neural Transm Suppl*. 10.1007/978-3-7091-6301-6_17

[54] Ogundele, O. M., Pardo, J., Francis, J., Goya, R. G., and Lee, C. C. (2018) A Putative Mechanism of Age-Related Synaptic Dysfunction Based on the Impact of IGF-1 Receptor Signaling on Synaptic CaMKIIalpha Phosphorylation. *Front Neuroanat*. **12**, 35

[55] Krabbe, K. S., Nielsen, A. R., Krogh-Madsen, R., Plomgaard, P., Rasmussen, P., et al. (2007) Brain-derived neurotrophic factor (BDNF) and type 2 diabetes. *Diabetologia*. **50**, 431–438

[56] Yamazaki, M., Yamada, H., Munetsuna, E., Ishikawa, H., Mizuno, G., et al. (2018)

Excess maternal fructose consumption impairs hippocampal function in offspring via epigenetic modification of BDNF promoter. *FASEB J.* **32**, 2549–2562

[57] Pinto, J. G., Jones, D. G., and Murphy, K. M. (2013) Comparing development of synaptic proteins in rat visual, somatosensory, and frontal cortex. *Front Neural Circuits*. **7**, 97

[58] Fingerle-Rowson, G., Petrenko, O., Metz, C. N., Forsthuber, T. G., Mitchell, R., et al. (2003) The p53-dependent effects of macrophage migration inhibitory factor revealed by gene targeting. *Proc Natl Acad Sci U S A.* **100**, 9354–9359

[59] Mamikutty, N., Thent, Z. C., Sapri, S. R., Sahruddin, N. N., Mohd Yusof, M. R., et al. (2014) The establishment of metabolic syndrome model by induction of fructose drinking water in male Wistar rats. *Biomed Res Int*. **2014**, 263897

[60] Teofilovic, A., Brkljacic, J., Djordjevic, A., VojnovicMilutinovic, D., Tappy, L., et al. (2020) Impact of insulin and glucocorticoid signalling on hepatic glucose homeostasis in the rat exposed to high-fructose diet and chronic stress. *Int J Food Sci Nutr*. **71**, 1–11

[61] Hammond, R. S., Tull, L. E., and Stackman, R. W. (2004) On the delay-dependent involvement of the hippocampus in object recognition memory. *Neurobiol. Learn. Mem.* **82**, 26–34

[62] Tanabe, M., Matsumoto, T., Shibuya, K., Tateda, K., Miyazaki, S., et al. (2005) Compensatory response of IL-1 gene knockout mice after pulmonary infection with Klebsiella pneumoniae. *J Med Microbiol*. **54**, 7–13

[63] Vujicic, M., Saksida, T., Despotovic, S., Bajic, S. S., Lalic, I., et al. (2018) The Role

of Macrophage Migration Inhibitory Factor in the Function of Intestinal Barrier. *Sci Rep*. **8**, 6337

[64] Morganti, J. M., Riparip, L. K., and Rosi, S. (2016) Call off the dog(ma): M1/M2 polarization is concurrent following traumatic brain injury. *PLoS One*. **11**, e0148001

[65] Crain, J. M., Nikodemova, M., and Watters, J. J. (2013) Microglia express distinct M1 and M2 phenotypic markers in the postnatal and adult central nervous system in male and female mice. *J. Neurosci. Res.* **91**, 1143–1151

[66] Orihuela, R., McPherson, C. A., and Harry, G. J. (2016) Microglial M1/M2 polarization and metabolic states. *Br. J. Pharmacol.* **173**, 649–665

[67] Ortega-Gómez, A., Perretti, M., and Soehnlein, O. (2013) Resolution of inflammation: An integrated view. *EMBO Mol. Med.* **5**, 661–674

[68] Spadaro, O., Camell, C. D., Bosurgi, L., Nguyen, K. Y., Youm, Y. H., et al. (2017) IGF1 Shapes Macrophage Activation in Response to Immunometabolic Challenge. *Cell Rep*. **19**, 225–234

[69] Tang, Y., and Le, W. (2016) Differential Roles of M1 and M2 Microglia in Neurodegenerative Diseases. *Mol Neurobiol*. **53**, 1181–1194

[70] Medina, E. A., Afsari, R. R., Ravid, T., Castillo, S. S., Erickson, K. L., et al. (2005) Tumor necrosis factor-{alpha} decreases Akt protein levels in 3T3-L1 adipocytes via the caspase-dependent ubiquitination of Akt. *Endocrinology*. **146**, 2726–2735

[71] Sajan, M., Hansen, B., Ivey 3rd, R., Sajan, J., Ari, C., et al. (2016) Brain Insulin Signaling Is Increased in Insulin-Resistant States and Decreases in FOXOs and PGC-1alpha and Increases in Abeta1-40/42 and Phospho-Tau May Abet Alzheimer

Development. *Diabetes*. **65**, 1892–1903

[72] Konner, A. C., and Bruning, J. C. (2012) Selective insulin and leptin resistance in metabolic disorders. *Cell Metab*. **16**, 144–152

[73] Djordjevic, A., Bursać, B., Veličković, N., Gligorovska, L., Ignjatović, D., et al. (2017) Disturbances of systemic and hippocampal insulin sensitivity in macrophage migration inhibitory factor (MIF) knockout male mice lead to behavioral changes associated with decreased PSA-NCAM levels. *Horm. Behav.* **96**, 95–103

[74] Wrigley, S., Arafa, D., and Tropea, D. (2017) Insulin-Like Growth Factor 1: At the Crossroads of Brain Development and Aging. *Front Cell Neurosci*. **11**, 14

[75] Barrett, J. P., Minogue, A. M., Falvey, A., and Lynch, M. A. (2015) Involvement of IGF-1 and Akt in M1/M2 activation state in bone marrow-derived macrophages. *Exp Cell Res*. **335**, 258–268

[76] Alboni, S., Poggini, S., Garofalo, S., Milior, G., El Hajj, H., et al. (2016) Fluoxetine treatment affects the inflammatory response and microglial function according to the quality of the living environment. *Brain Behav Immun*. **58**, 261–271

[77] Lu, B., Pang, P. T., and Woo, N. H. (2005) The yin and yang of neurotrophin action. *Nat Rev Neurosci*. **6**, 603–614

[78] Coley, A. A., and Gao, W. J. (2019) PSD-95 deficiency disrupts PFC-associated function and behavior during neurodevelopment. *Sci Rep*. **9**, 9486

[79] Feyder, M., Karlsson, R. M., Mathur, P., Lyman, M., Bock, R., et al. (2010) Association of mouse Dlg4 (PSD-95) gene deletion and human DLG4 gene variation with phenotypes relevant to autism spectrum disorders and Williams' syndrome. *Am*

J Psychiatry. **167**, 1508–1517

[80] Krishnan, M. L., Van Steenwinckel, J., Schang, A. L., Yan, J., Arnadottir, J., et al. (2017) Integrative genomics of microglia implicates DLG4 (PSD95) in the white matter development of preterm infants. *Nat Commun*. **8**, 428

[81] Granja, M. G., Alves, L. P., Leardini-Tristao, M., Saul, M. E., Bortoni, L. C., et al. (2021) Inflammatory, synaptic, motor, and behavioral alterations induced by gestational sepsis on the offspring at different stages of life. *J Neuroinflammation*. **18**, 60

[82] Zalcman, G., Federman, N., and Romano, A. (2018) CaMKII Isoforms in Learning and Memory: Localization and Function. *Front Mol Neurosci*. **11**, 445

[83] Tremblay, F., Brûlé, S., Sung, H. U., Li, Y., Masuda, K., et al. (2007) Identification of IRS-1 Ser-1101 as a target of S6K1 in nutrient- and obesity-induced insulin resistance. *Proc. Natl. Acad. Sci. U. S. A.* **104**, 14056–14061

[84] Spagnuolo, M. S., Iossa, S., and Cigliano, L. (2021) Sweet but bitter: Focus on fructose impact on brain function in rodent models. *Nutrients*. **13**, 1–18

[85] Xu, M. X., Yu, R., Shao, L. F., Zhang, Y. X., Ge, C. X., et al. (2016) Up-regulated fractalkine (FKN) and its receptor CX3CR1 are involved in fructose-induced neuroinflammation: Suppression by curcumin. *Brain Behav Immun*. **58**, 69–81

[86] Alva, N., Alva, R., and Carbonell, T. (2016) Fructose 1,6-Bisphosphate: A Summary of Its Cytoprotective Mechanism. *Curr Med Chem*. **23**, 4396–4417

[87] Oppelt, S. A., Zhang, W., and Tolan, D. R. (2017) Specific regions of the brain are capable of fructose metabolism. *Brain Res*. **1657**, 312–322

[88] Cardenas, A., Hurtado, O., Leza, J. C., Lorenzo, P., Bartrons, R., et al. (2000) Fructose-1,6-bisphosphate inhibits the expression of inducible nitric oxide synthase caused by oxygen-glucose deprivation through the inhibition of glutamate release in rat forebrain slices. *Naunyn Schmiedebergs Arch Pharmacol*. **362**, 208–212

[89] Seok, S. M., Park, T. Y., Park, H. S., Baik, E. J., and Lee, S. H. (2015) Fructose-1,6-bisphosphate suppresses lipopolysaccharide-induced expression of ICAM-1 through modulation of toll-like receptor-4 signaling in brain endothelial cells. *Int Immunopharmacol*. **26**, 203–211

[90] Djordjevic, A., Bursać, B., Veličković, N., Vasiljević, A., and Matić, G. (2015) The impact of different fructose loads on insulin sensitivity, inflammation, and PSA-NCAM-mediated plasticity in the hippocampus of fructose-fed male rats. *Nutr. Neurosci.* **18**, 66–75

[91] Bay-Richter, C., Janelidze, S., Sauro, A., Bucala, R., Lipton, J., et al. (2015) Behavioural and neurobiological consequences of macrophage migration inhibitory factor gene deletion in mice. *J Neuroinflammation*. **12**, 163

[92] Molteni, R., Barnard, R. J., Ying, Z., Roberts, C. K., and Gomez-Pinilla, F. (2002) A high-fat, refined sugar diet reduces hippocampal brain-derived neurotrophic factor, neuronal plasticity, and learning. *Neuroscience*. **112**, 803–814

[93] Shaker, O. G., Sourour, D. A., and Taha, M. (2009) Effects of Statins on Insulin-Like Growth Factor-1 Gene Expression in Fructose Induced Metabolic Syndrome in Rats. *Open Endocrinol. J.* **3**, 28–33

[94] Erlanson-Albertsson, C., and Lindqvist, A. (2010) Fructose affects enzymes

involved in the synthesis and degradation of hypothalamic endocannabinoids. *Regul Pept*. **161**, 87–91

[95] Franco-Perez, J., Manjarrez-Marmolejo, J., Ballesteros-Zebadua, P., Neri-Santos, A., Montes, S., et al. (2018) Chronic Consumption of Fructose Induces Behavioral Alterations by Increasing Orexin and Dopamine Levels in the Rat Brain. *Nutrients*. 10.3390/NU10111722

[96] Zanettini, C., Panlilio, L. V, Alicki, M., Goldberg, S. R., Haller, J., et al. (2011) Effects of endocannabinoid system modulation on cognitive and emotional behavior. *Front Behav Neurosci*. **5**, 57

[97] Beck, Gc., Brinkkoetter, P., Hanusch, C., Schulte, J., van Ackern, K., et al. (2004) Clinical review: immunomodulatory effects of dopamine in general inflammation. *Crit Care*. **8**, 485–491

[98] Felger, J. C., Li, Z., Haroon, E., Woolwine, B. J., Jung, M. Y., et al. (2016) Inflammation is associated with decreased functional connectivity within corticostriatal reward circuitry in depression. *Mol Psychiatry*. **21**, 1358–1365

[99] Kringelbach, M. L., and Berridge, K. C. (2010) The Neuroscience of Happiness and Pleasure. *Soc Res (New York)*. **77**, 659–678

[100] De Macedo, I. C., De Freitas, J. S., and Da Silva Torres, I. L. (2016) The influence of palatable diets in reward system activation: A mini review. *Adv. Pharmacol. Sci.* 10.1155/2016/7238679

[101] Horst, N. K., and Laubach, M. (2013) Reward-related activity in the medial prefrontal cortex is driven by consumption. *Front. Neurosci.* **0**, 56

Figure captions

Figure 1. Markers of inflammation. (A) Representative Western blots and relative quantification of **(B)** pIκB^{Ser32}, total IκB, their ratio and NF-κB/p65 protein level **(C)** F4/80 protein level and **(D)** relative mRNA levels of *Arg-1*, *Lif* and *Mrc-1* in the PFC of C57BL/6J mice (WT), mice with genetically deleted *Mif* (MIF-KO), MIF-KO mice on fructose diet (MIF-KO+F) and WT mice on fructose diet (WT + F). Immunoreactivities of analyzed samples were normalized to β-actin as a loading control, while HPRT1 was used as endogenous control for the PCR analysis. The data are presented as mean ± SEM (n = 6 – 8 animals per group). A value of $p<0.05$ was considered statistically significant. Significant between-group differences from post-hoc Tukey test are given as follows: **$p<0.01$, ***$p<0.001$, all groups *vs.* WT; $^{###}p<0.001$, MIF-KO + F vs. MIF-KO.

Figure 2. Insulin signaling. Representative Western blots and relative quantification of IR, pIRS-1^{Ser307}, pIRS-1^{Ser1101} and IRS-1 and their ratios in the PFC of C57BL/6J mice (WT), mice with genetically deleted *Mif* (MIF-KO), MIF-KO mice on fructose diet (MIF-KO+F) and WT mice on fructose diet (WT + F). Immunoreactivities of analyzed samples were normalized to β-actin as a loading control. The data are presented as mean ± SEM (n = 6 – 8 animals per group). A value of $p<0.05$ was considered statistically significant. Significant between-group differences from post-hoc Tukey test are given as follows: **$p<0.01$, ***$p<0.001$, all groups *vs.* WT; $^{\dagger}p<0.05$, MIF-KO + F vs. WT + F.

Figure 3. Markers of insulin resistance and energy balance. Representative Western blots

and relative quantification of **(A)** pPKCα^{Ser657}, PKCα and their ratio; **(B)** pAkt1/2/3^{Ser473}, total Akt1/2/3 and their ratio; **(C)** pGSK-3β^{Ser9}, GSK-3β and their ratio and **(D)** pAMPKα^{Thr172}, total AMPKα and their ratio in the PFC of C57BL/6J mice (WT), mice with genetically deleted *Mif* (MIF-KO), MIF-KO mice on fructose diet (MIF-KO+F) and WT mice on fructose diet (WT + F). Immunoreactivities of analyzed samples were normalized to β-actin as a loading control. The data are presented as mean ± SEM (n = 6 – 8 animals per group). A value of $p<0.05$ was considered statistically significant. Significant between-group differences from post-hoc Tukey test are given as follows: *$p<0.05$, **$p<0.01$, ***$p<0.001$, all groups *vs.* WT; $^{\#\#}p<0.01$, MIF-KO + F vs. MIF-KO.

Figure 4. Glucocorticoid signaling. Representative Western blots and relative quantification of 11β-HSD1, pGR^{Ser220} , GR and their ratio in the PFC of C57BL/6J mice (WT), mice with genetically deleted *Mif* (MIF-KO), MIF-KO mice on fructose diet (MIF-KO+F) and WT mice on fructose diet (WT + F). Immunoreactivities of analyzed samples were normalized to β-actin as a loading control. The data are presented as mean ± SEM (n = 6 – 8 animals per group). A value of $p<0.05$ was considered statistically significant. Significant between-group differences from post-hoc Tukey test are given as follows: **$p<0.01$, WT + F *vs.* WT; $^{\dagger\dagger}p<0.01$, MIF-KO + F vs. WT + F.

Figure 5. Synaptic plasticity markers. (A) Representative Western blots and relative quantification of **(B)** pCaMKII^{Thr286}, total CaMKII and their ratio; **(C)** PSD-95 and synaptophysine protein levels and **(D)** relative mRNA levels for *Bdnf-9* and *Igf-1* in the PFC

of C57BL/6J mice (WT), mice with genetically deleted *Mif* (MIF-KO), MIF-KO mice on fructose diet (MIF-KO+F) and WT mice on fructose diet (WT + F). Immunoreactivities of analyzed samples were normalized to β-actin as a loading control, while HPRT1 was used as endogenous control for the PCR analysis. The data are presented as mean ± SEM (n = 6 – 8 animals per group). A value of $p<0.05$ was considered statistically significant. Significant between-group differences from post-hoc Tukey test are given as follows: $^{**}p<0.01$, $^{***}p<0.001$, all groups *vs.* WT; $^{\#}p<0.05$, $^{\#\#}p<0.01$, $^{\#\#\#}p<0.001$, MIF-KO + F vs. MIF-KO; $^{\dagger\dagger\dagger}p<0.01$, MIF-KO + F vs. WT + F.

Figure 6. Behavioral tests. (A) Latency to enter OA and **(B)** % of total crossings into OA in the elevated plus maze (EPM) test; **(C)** Latency to enter dark box and **(D)** time spent in dark in the light dark box (LDB) test; **(D)** Novel object preference ratio expressed as % of exploration time in the NOR test are shown for C57BL/6J mice (WT), mice with genetically deleted *Mif* (MIF-KO), MIF-KO mice on fructose diet (MIF-KO+F) and WT mice on fructose diet (WT + F). Data are presented as mean ± SEM (n = 8 animals per group). Significant between-group differences from post hoc Tukey test are given as follows: $^{*}p < 0.05$, MIF-KO vs. WT; $^{\#}p < 0.05$, MIF-KO+F vs. MIF-KO.

This is the peer reviewed version of the following article: Vratarić M, Šenk V, Bursać B, Gligorovska L, Ignjatović D, Kovačević S, Veličković N, Djordjevic A. Fructose diet ameliorates effects of macrophage migration inhibitory factor deficiency on prefrontal cortex inflammation, neural plasticity, and behavior in male mice. Biofactors. 2021, which has been published in final form at http://dx.doi.org/10.1002/biof.1802.

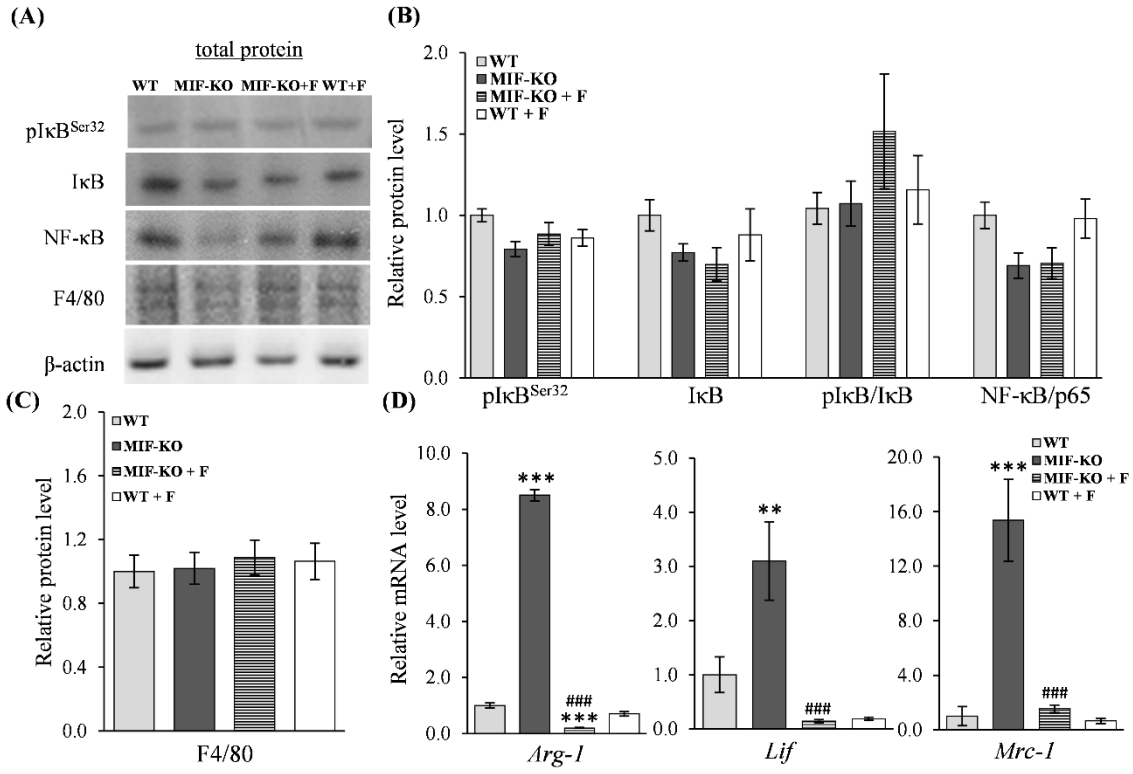

Figure 1.

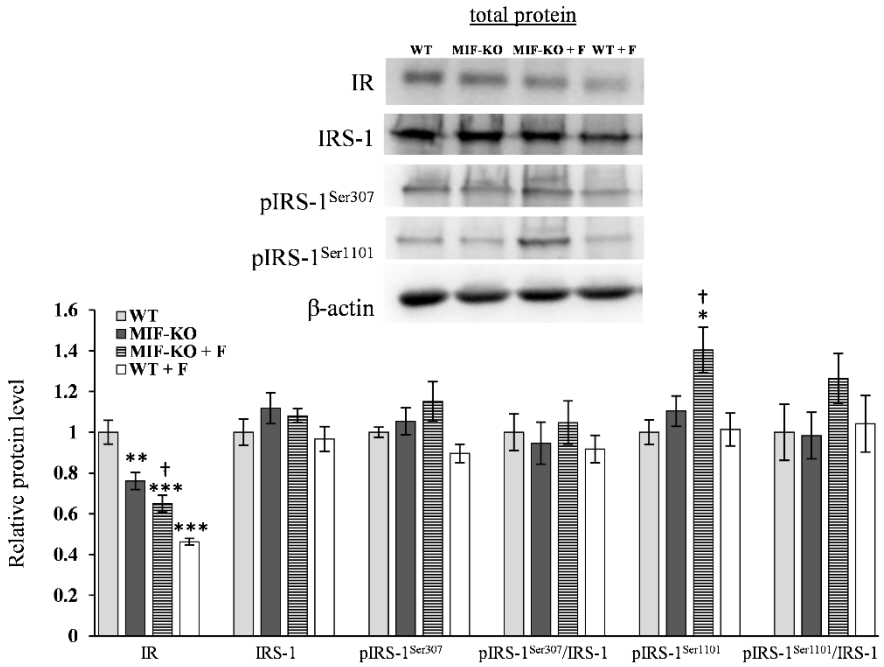

Figure 2.

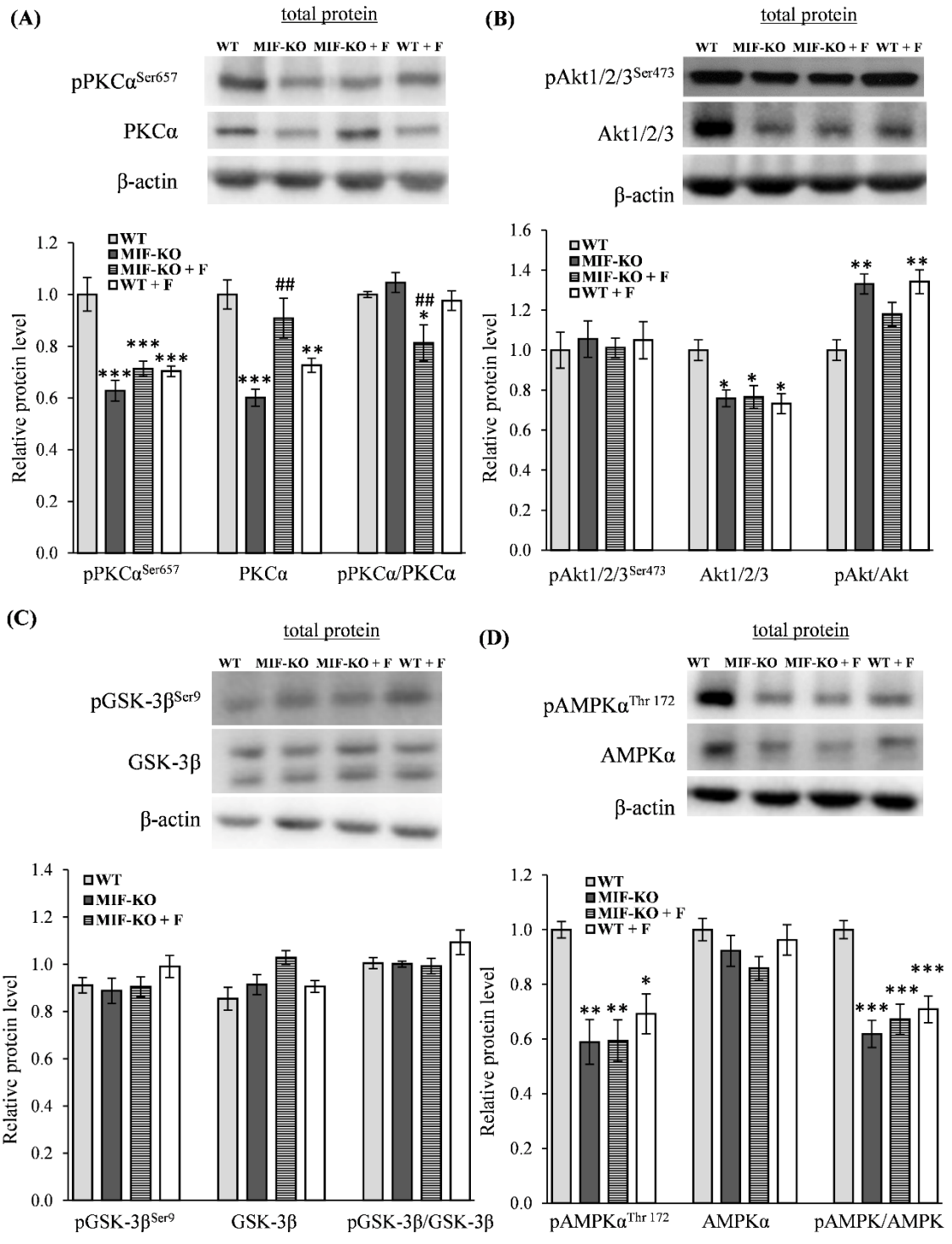

Figure 3.

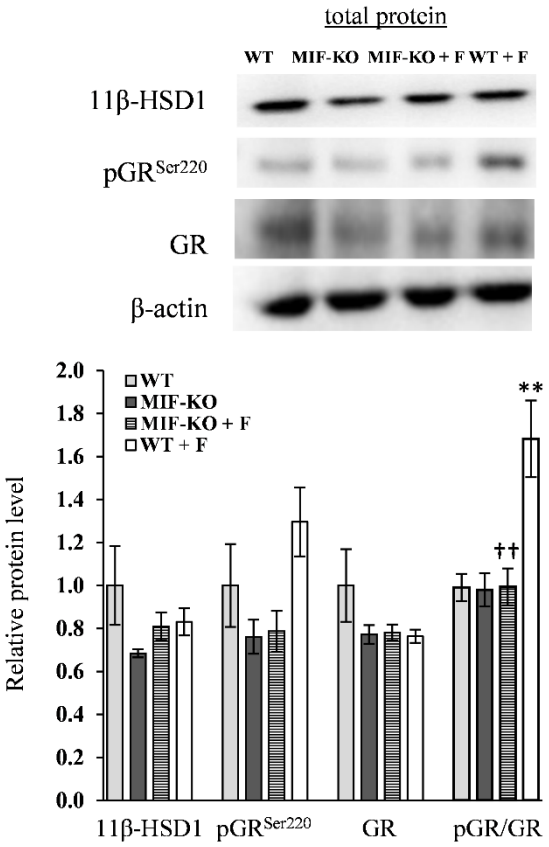

Figure 4.

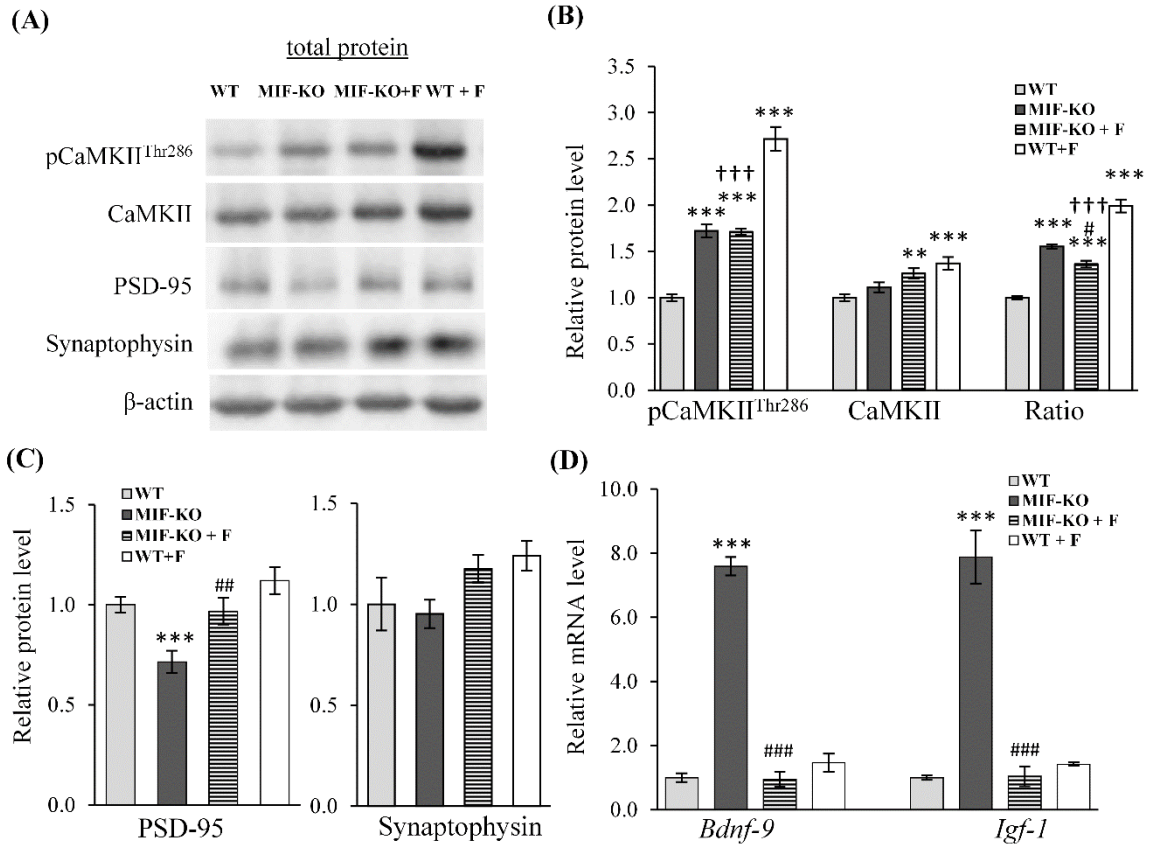

Figure 5.

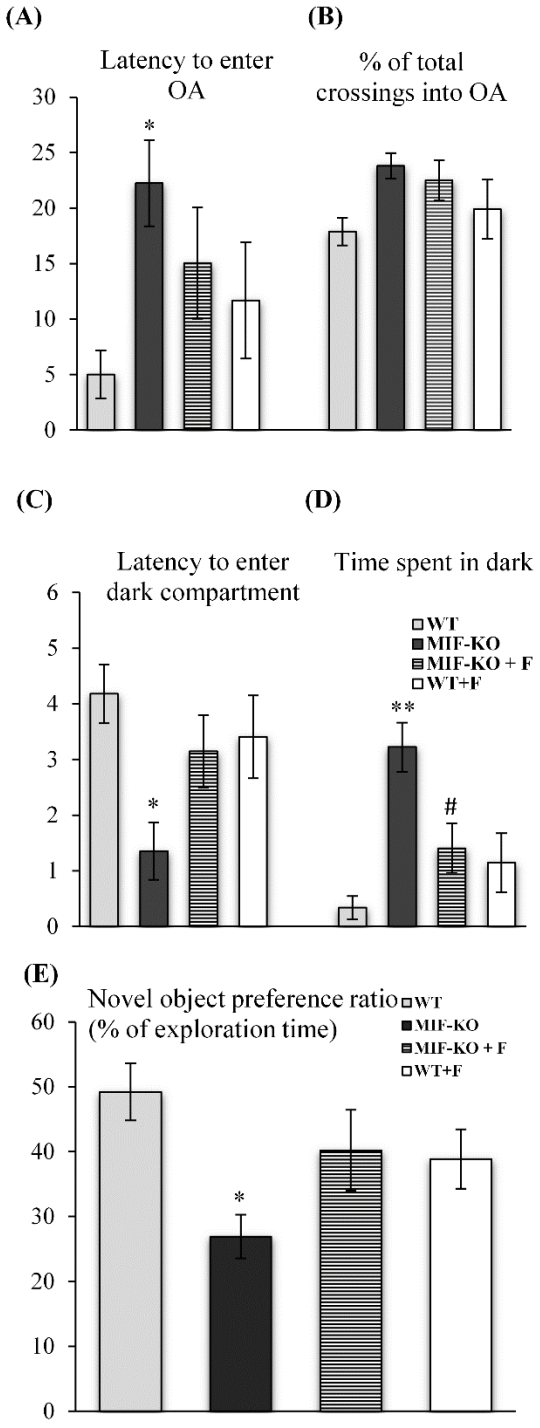

Figure 6.